Surface & Coatings Technology xxx (2010) xxx–xxx

Contents lists available at ScienceDirect

Surface & Coatings Technology

journal homepage: www.elsevier.com/locate/surfcoat

Singlet oxygen generating nanolayer coatings on NiTi alloy for photodynamic application

Kyong-Hoon Choi [a], Kang-Kyun Wang [a], Seung-Lim Oh [a], Ji-Eun Im [a], Bong-Jin Kim [a], Jong-Chul Park [b], DongHoon Choi [c], Hwan-Kyu Kim [d], Yong-Rok Kim [a,*]

[a] Department of Chemistry, Yonsei University, Seoul 120-749, Republic of Korea
[b] Department of Medical Engineering, Yonsei University College of Medicine, Seoul 120-752, Republic of Korea
[c] Cardiology Division, Yonsei Cardiovascular Center, Yonsei University College of Medicine, Seoul 120-752, Republic of Korea
[d] Department of Advanced Material Chemistry, Korea University, Jochiwon, Chungnam 339-700, Republic of Korea

ARTICLE INFO

Article history:
Received 19 September 2009
Accepted in revised form 13 April 2010
Available online xxxx

Keywords:
Singlet oxygen
NiTi alloy
Photodynamic therapy
Photosensitizer
Esterification

ABSTRACT

Photodynamic Therapy (PDT) is a promising approach for killing microorganism and especially for the inactivation of antibiotic-resistant strains. The photodynamic process rapidly generates reactive oxygen species (ROS) as for instance peroxides, hydroxyl radicals, superoxide ions, and singlet oxygen. Among them, the singlet oxygen is considered to be a major causative agent of cellular damage in photodynamic process. Due to advantage of the cytotoxic effect of PDT on bacteria, the PDT method has been one of the most appropriate tools to prevent the microbes which result in biofilm formation. This work describes a method of singlet oxygen generating nanolayer coating on NiTi alloy which shows a good biocompatibility. The 5,10,15-triphenyl-20-(4-carboxyphenyl)-porphyrin] platinum (PtCP) functional nanolayer coatings were prepared in two steps. In the first step, Al coating was prepared on biomedical NiTi alloy substrate by DC magnetron sputtering, and then this coated substrate alloy was immersed into hot water to form Al_2O_3 coatings. In the second step, a photosensitizer (PS) with carboxyl group was chemically attached to the hydroxyl-terminated Al_2O_3 coatings by a direct esterification method. The microstructure and the elemental and phase composition of the coating were investigated by scanning electron microscopy (SEM), energy dispersive X-ray spectrometer (EDS), and X-ray diffraction (XRD). Results from this study show that the PtCP functional nanolayer coating is composed of many perpendicular nanosheet structures. These very thin nanosheet structures with the thickness of a few nanometers mainly show amorphous phase. The singlet oxygen generation efficiency of the PS being chemically bonded on these nanosheets was detected by an indirect chemical method by using the decomposition of 1,3-diphenyl-isobenzofuran (DPBF).

1. Introduction

Over the last decade, PDT has been used to be a light-activated new modality to treat diseases ranging from cancer to antibiotic-resistant infections [1–4]. PDT combines a nontoxic PS and harmless visible light to produce reactive oxygen species that can kill mammalian and microbial cells. During PDT, the delivery of visible light at the appropriate wavelength is necessary to excite the PS molecule to higher excited singlet state. This excited state may then undergo intersystem crossing to the slightly lower energy, but longer-lived triplet state. This triplet state of the PS can either interact with oxygen to produce singlet oxygen (Type II reaction) or directly react with the molecules near the immediate vicinity (Type I reaction) [5–10]. Although the bacterial killing can be mediated by either of the above mentioned reactions, it is known that the singlet oxygen is the predominant chemical entity causing cell death. Recently, a series of researches have shown that it is possible to kill bacteria by using ROS that is generated from photosensitizers such as methylene blue (MB) or toluidine blue O (TBO) [11–14]. In addition, bacteria, as well as fungi, yeasts, and viruses, treated with photosensitizers were shown to be successfully killed by visible light [15].

NiTi alloy has been one of the most popular metallic implant materials due to its unique properties such as shape memory effect, superelastic properties, good biocompatibility, cytotoxicity and high corrosion resistance [16,17]. These novel properties enable it to be widely used in industrial applications as well as medical and dental applications [18]. Therefore, technology of PDT agent coatings on biocompatible material is becoming a very important because these functional materials can prevent the microbes which result in biofilm formation and infections.

In the present study, we have come up with a new method to fabricate the singlet oxygen generating nanolayer coatings on

* Corresponding author. Tel.: +82 2 2123 2646; fax: +82 2 364 7050.
E-mail address: yrkim@yonsei.ac.kr (Y.-R. Kim).

0257-8972/$ – see front matter © 2010 Elsevier B.V. All rights reserved.
doi:10.1016/j.surfcoat.2010.04.033

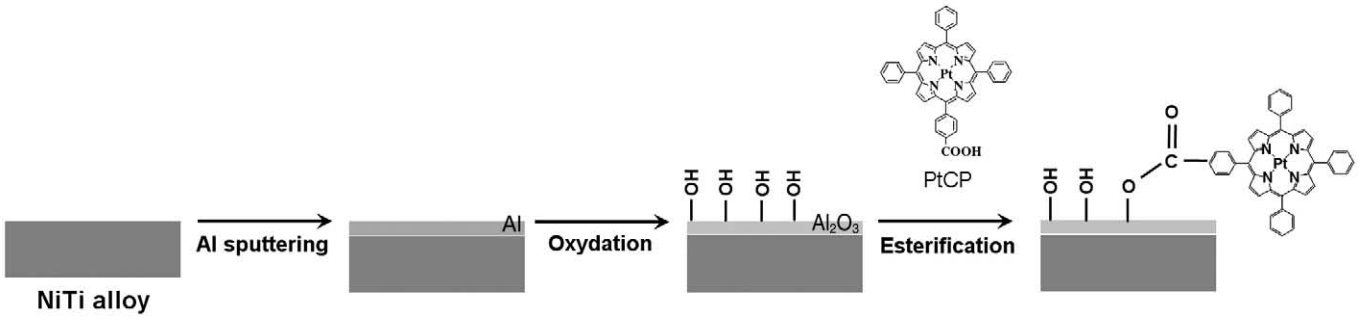

Scheme 1. Fabrication procedure of singlet oxygen generating nanolayer coatings on NiTi alloy.

biomedical NiTi alloy. First, Al_2O_3 coating was deposited on NiTi alloy substrate by DC magnetron sputtering and oxidation process. And then the PtCP molecules with carboxyl group were chemically attached to the hydroxyl-terminated Al_2O_3 coatings by a direct esterification method.

2. Experimental

2.1. Preparation of the PtCP functional nanolayer coatings

A commercial NiTi alloy (Beijing Gee SMA Technology Co. Ltd, China) with the composition of Ni–51.83Ti–48.17 at.% was cut into samples of 9 mm in diameter and 0.2 mm thickness for the substrate material. The surface was cleaned ultrasonically in acetone and distilled water and then dried at 90 °C. Al coating was deposited on NiTi alloy substrate by DC magnetron sputtering by using the metallic aluminum (99.99%) target. The distance between the target and the substrate was 10 cm. The vacuum chamber was pumped down to the pressure of 1.0×10^{-5} Pa. During the coating deposition, flow of Ar gas was kept constantly at 30 sccm. The direct current (DC) sputtering power applied on the target was maintained at 300 W and the substrate temperature was at room temperature. To oxidize the Al coatings, the Al sputtered NiTi alloy was immersed into hot water at 90 °C for 90 min. After washing and drying, Al_2O_3 coated NiTi alloy was immersed in 10 mL of 2.0×10^{-5} M PtCP/toluene solution and introduced into a shaking water bath. The speed and temperature of the shaker water bath were maintained at 100 rpm and 40 °C, respectively, for 24 h. After 24 h, Al_2O_3 coated NiTi alloy was cleaned using toluene and distilled water. PtCP was synthesized as previously described [19].

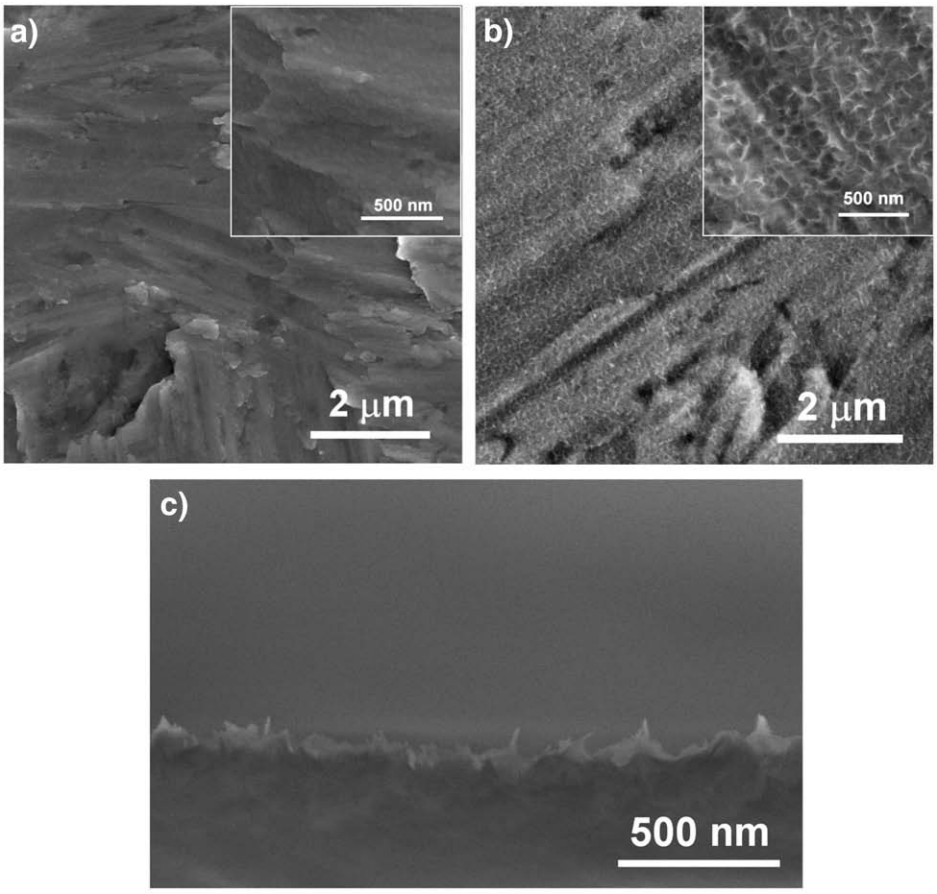

Fig. 1. FE-SEM images of the surface and cross-sectional morphologies of (a) Al coating before oxidation reaction and (b,c) after oxidation reaction of Al coatings at 90 °C for 90 min. The inset represents the high magnification image.

Please cite this article as: K.-H. Choi, et al., Surf. Coat. Technol. (2010), doi:10.1016/j.surfcoat.2010.04.033

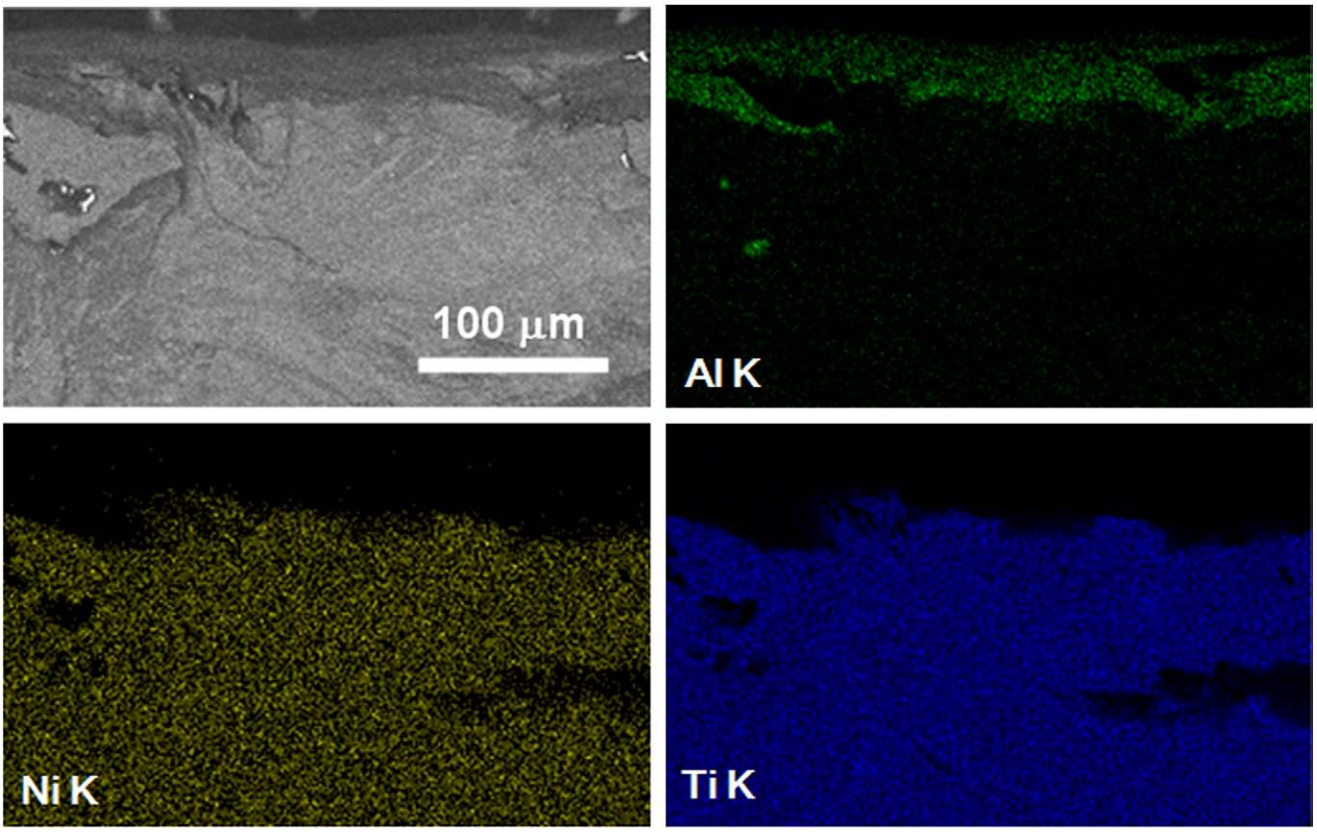

Fig. 2. Micrograph and elemental X-ray maps of a cross-section of the Al_2O_3 coating on NiTi alloy.

2.2. Detection of singlet oxygen

The degradation of DPBF as a singlet oxygen quencher was studied for the functional nanolayer coated NiTi alloy. In a typical experiment, a 3.5 mL of THF solution containing the functional nanolayer coated NiTi alloy and DPBF (1.0×10^{-5} M) was introduced to a 1 cm quartz cell in the dark. The Xe lamp (150 W, Abet Technologies, USA) was used as the irradiation source. A 480 nm glass cut off filter was used to filter off ultraviolet light, so that only the porphyrin Q band was irradiated, which prevents direct photodegradation of DPBF by UV light irradiation. At every 2 min of irradiation, the absorption spectra of the samples were monitored by means of a UV–Vis spectrophotometer.

2.3. Characterization of the PtCP functional nanolayer coatings

The surface morphology and topography of the functional nanolayer coated NiTi alloy were observed by field emission scanning electron microscopy (FESEM, Hitachi, SU–70, KBSI Gangneung Center) equipped with an energy dispersive X-ray spectroscopy (EDS) and transmission electron microscopy (TEM, JEOL JEM-2100F), respectively. The crystallographic characteristics and nanostructure of the composite coatings were investigated with X-ray diffractometer (PANalytical, X'Pert Pro MPD) working on Cu Kα radiation. Infrared spectra were obtained using a PerkinElmer FT-IR spectrum 100 spectrometer. For IR measurements, samples were crushed in an agate mortar and then prepared in the form of pressed wafers (ca. 1% sample in KBr). Absorption and emission spectra were obtained from a diffuse reflectance UV–Vis spectrophotometer (Jasco V-550) equipped with an integrating sphere (Jasco ISV-469) and spectrofluorometer (Hitachi, F-4500), respectively.

3. Results and discussion

The singlet oxygen generating nanolayer coatings were prepared by a simple surface modification process with which PtCP was covalently bonded to Al_2O_3 coatings to yield the PtCP functional nanolayer coatings as shown in Scheme 1. The coated Al_2O_3 on NiTi alloy substrate was prepared by DC magnetron sputtering and oxidation process. PtCP molecules were then chemically bonded to Al_2O_3 coating by a direct esterification. The coated NiTi alloy substrate showed a metallic silver color after Al_2O_3 coating process and subsequently it changed into reddish silver color after the esterificated reaction with PtCP molecules.

Fig. 1a and b shows the difference of the surface morphologies of the Al coatings before oxidation reaction and after oxidation reaction

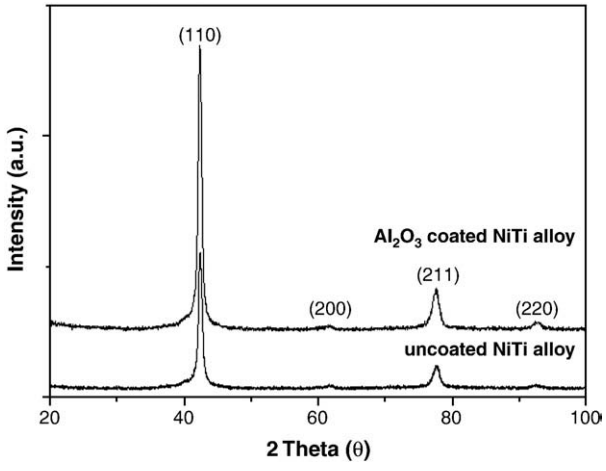

Fig. 3. XRD patterns of uncoated NiTi alloy and Al_2O_3 coated NiTi alloy.

Please cite this article as: K.-H. Choi, et al., Surf. Coat. Technol. (2010), doi:10.1016/j.surfcoat.2010.04.033

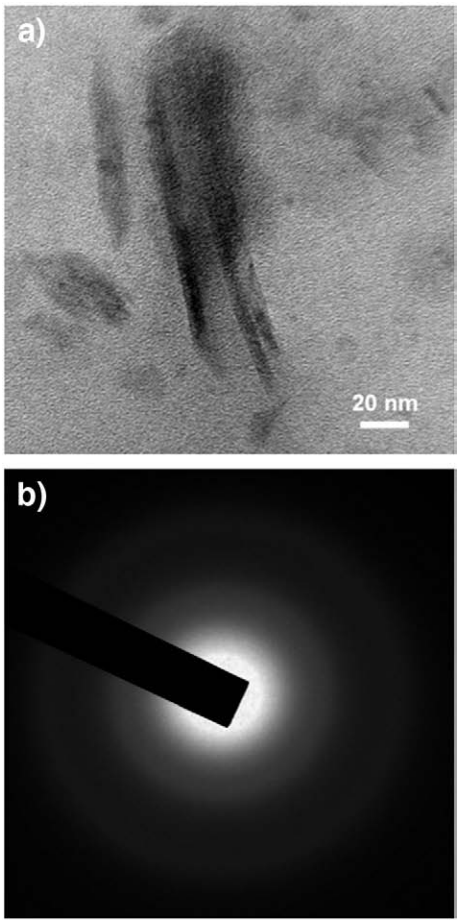

Fig. 4. (a) HR-TEM images of the niddle-like nanosheet structure which is fabricated by the hot water treatment of Al coatings. (b) Electron diffraction pattern for a selected area of the nanosheet structures.

of sputtered Al coatings respectively. The high magnification image of Fig. 1a indicates that the Al coating surface exhibits "mud-crack" or "segmented" morphology with the nanosized grains being well separated and homogeneously distributed over the surface. From Fig. 1b, it is observed that the coatings have the perpendicular nanosheet structure such as porous and coarsely needle-like morphologies, which are fabricated by the hot water treatment of Al coating. The nanosheet structure consists of needle-like morphologies with a size of about 100 nm. Also, the cross-sectional morphology (Fig. 1c) of the Al_2O_3 nanosheet coating shows the coating thickness of about 170 nm. Therefore, such nanocomposite coating fabricated by this process can provide a large surface area in order to have more PtCP molecules bonded to the surface. Even after an esterificated reaction with PtCP, the nanocomposite coatings are still maintained as the nanosheet structure.

Fig. 2 displays the micrograph and elemental X-ray maps of a cross-section of the Al_2O_3 coated NiTi alloy obtained after oxidation in hot water at 90 °C for 90 min. It shows that the nanocomposite coated NiTi alloy is composed of Al, Ni, and Ti. The topcoat layer is mainly composed of aluminum and the substrate layer is mainly composed of Ni and Ti.

Since the thickness of the Al_2O_3 nanosheet coating is less than 1 μm, the XRD provides the structural information on both Al_2O_3 nanosheet coatings and NiTi alloy substrate. XRD spectra of the uncoated NiTi alloy and the Al_2O_3 nanosheet coated NiTi alloy are shown in Fig. 3. Four characteristic peaks ($2\theta = 42.31$, 61.88, 77.51, 92.36°), marked by their Miller indices ((110), (200), (211), and (220)) are observed in the case of NiTi alloy (JCPDS no. 18-0899). After Al_2O_3 coating, the XRD pattern has no significant change and no characteristic peaks for Al_2O_3 crystalline are observed. Because XRD pattern of the Al_2O_3 nanosheets is observed with the sample which is fabricated by following the procedure for the Al_2O_3 coating, it is suggested that the resultant Al_2O_3 nanosheets on the surface of NiTi alloy have the amorphous phase.

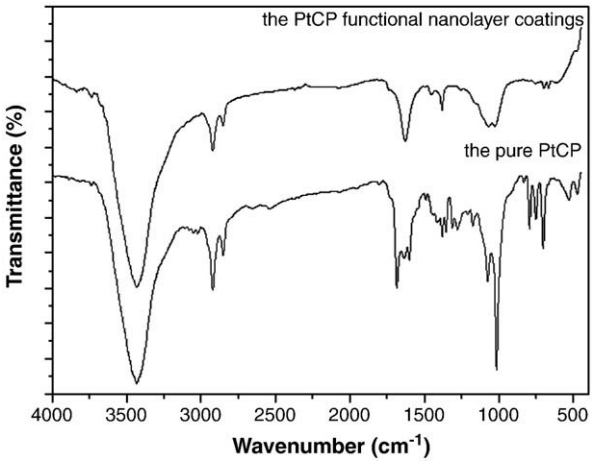

Fig. 5. FT-IR spectra of the pure PtCP and the PtCP functional nanolayer coating.

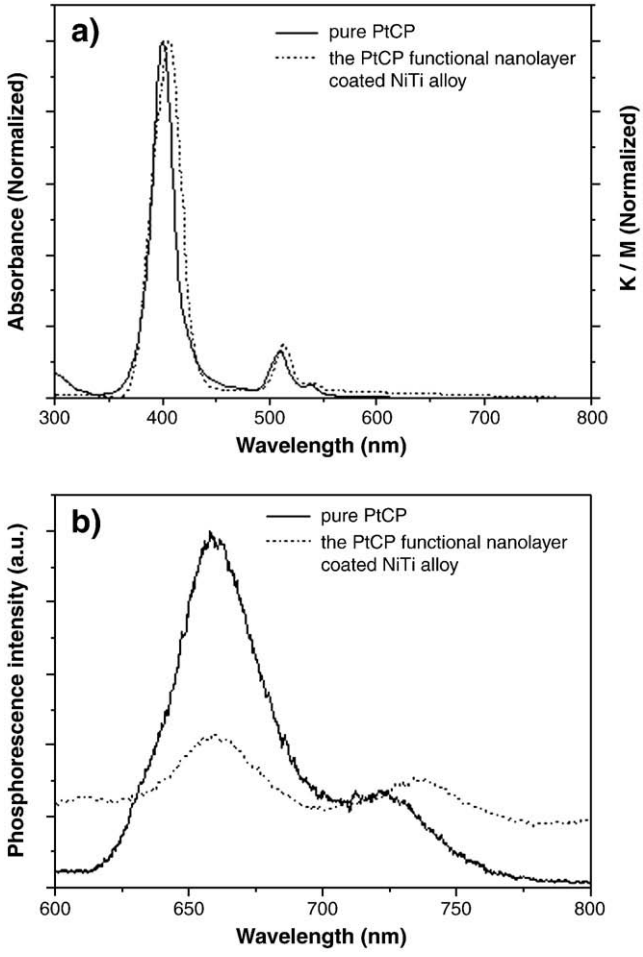

Fig. 6. (a) Absorption and (b) phosphorescence spectra of the pure PtCP in THF and the PtCP functional nanolayer coated NiTi alloy. The absorption spectrum of the functional nanolayer coated NiTi alloy is obtained by applying the Kubelka–Munk function to the diffuse reflectance spectrum. For comparison, the intensity of normal absorption spectrum of PtCP solution is normalized with the intensity of diffuse reflectance data of the functional nanolayer coated NiTi alloy. The excitation wavelength is 408 nm for the emission spectrum.

Please cite this article as: K.-H. Choi, et al., Surf. Coat. Technol. (2010), doi:10.1016/j.surfcoat.2010.04.033

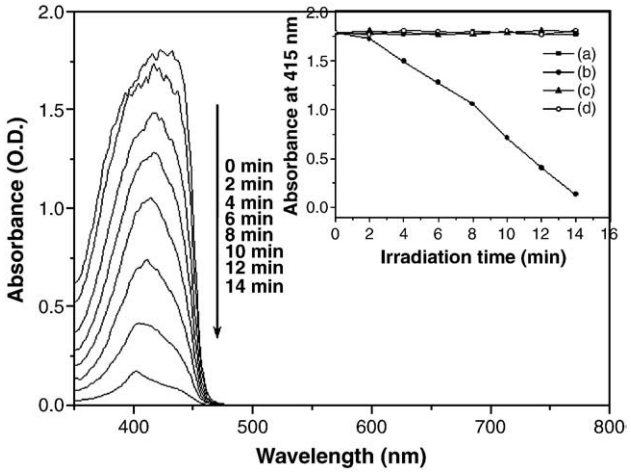

Fig. 7. Reaction time dependent UV–Vis spectra of DPBF in the presence of the PtCP functional nanolayer coated NiTi alloy in THF solution with light. The inset represents decay curves of DPBF absorption O.D. at 415 nm as a function of irradiation time. (a) DPBF only under the light, (b) DPBF with NiTi alloy with the PS under the light, (c) DPBF with NiTi alloy without the PS under the light, and (d) DPBF with NiTi alloy with the PS in the dark condition.

TEM image of the nanosheet structure, which is obtained from the Al_2O_3 coatings bonded with the PtCP, is shown in Fig. 4a. The very thin needle-like nanosheets with the thickness of several nanometers are presented. Fig. 4b is a selected area electron diffraction (SAED) pattern of the PtCP functional nanolayer coatings after the esterificated reaction of Al_2O_3 coatings. The nanosheet structure is not shown from this SAED pattern and the appeared faint ring pattern implies that the Al_2O_3 nanosheet structure is amorphous. This result is in agreement with the X-ray diffraction pattern. Also the high resolution TEM image of the needle-like nanosheet doesn't show any lattice fringe pattern as well.

Typical FT-IR spectra of the pure PtCP and the PtCP functional nanolayer coating bonded with PtCP are displayed in Fig. 5. The main bands of the PtCP functional nanolayer coatings are quite consistent with the main bands of the pure PtCP, showing almost the characteristic peaks of this compound. It indicates that PtCP molecules are still present on the surface of Al_2O_3 coatings even after being washed by toluene solvent. In particular, both samples show the intense peaks at 700, 752, 798, 1073 and 3054 cm^{-1} assigned to (C–H) stretching vibrations of phenyl and pyrrole rings [20–22]. Comparing FT-IR spectra of the pure PtCP and the PtCP functional nanolayer coatings, the pure PtCP has peaks at 3433 and 1687 cm^{-1} corresponding to a hydroxyl and carbonyl stretching of the carboxyl groups of PtCP. On the other hand, the PtCP functional nanolayer coating bonded with PtCP shows a strong and broad peak at 1629 cm^{-1} and a weak and broad peak at 1384 cm^{-1}. The peak of 1629 cm^{-1} is identified to be an asymmetric COO– stretch and that of 1384 cm^{-1} is identified as a symmetric COO– stretch [23,24]. They suggest that most of PtCP molecules are bound up with the surface of Al_2O_3 coating through the carboxyl group.

UV–Vis absorption and emission spectra of the pure PtCP and the functional nanolayer coated NiTi alloy are displayed in Fig. 6a and b, respectively. The diffuse reflectance spectra were translated into the absorption spectra by the Kubelka–Munk method [25]. The Kubelka–Munk equation is generally used for the analysis of diffuse reflectance spectra obtained from weakly absorbing samples. Kubelka–Munk's equation is described as follows:

$$\frac{K}{S} = \frac{(1-R)^2}{2R}$$

where K indicates the absorption coefficient, S and R represent the scattering coefficient and the absolute reflectance respectively. The UV–Vis absorption spectrum of the functional nanolayer coated NiTi alloy shows a similar pattern to the characteristics of the pure PtCP in THF. The peak at 400 nm is due to the Soret band of the pure PtCP, and the peaks due to the Q band are located at 510 nm and 538 nm. After the esterificated reaction with PtCP, the Soret band and Q bands exhibit a slight red-shift and broadness compared with the pure PtCP due to the inhomogeneous coupling with the Al_2O_3 surface. Being excited at the wavelength of 408 nm, the pure PtCP exhibits two strong emission peaks located at 660 and 725 nm. The functional nanolayer coated NiTi alloy also exhibited a red-shift and broadening compared with that of the pure PtCP, corresponding to the same phenomenon observed in the absorption.

As a specific singlet oxygen quencher, DPBF readily undergoes 1,4-cycloaddition reaction with singlet oxygen to form the endoperoxides, which in turn decomposes into the irreversible products (1,2-dibenzoylbenzene) [26]. DPBF reacts irreversibly with $^1O_2$ generated by photoexcitation of a PS and the reaction can easily be followed by measuring the decrease in optical density of the DPBF absorption at 415 nm [27]. Fig. 7 illustrates the changes in the absorption spectra of DPBF which depends on the reaction time with irradiation in the presence of the PtCP functional nanolayer coated NiTi alloy. The result indicates that the PtCP functional nanolayer coated NiTi alloy efficiently degraded the DPBF solution only under the light, while the thermal decomposition of DPBF was not observed.

4. Conclusions

In the present study, the singlet oxygen generating nanolayer coating is successfully prepared on biocompatible NiTi alloy by simple surface modification process of DC magnetron sputtering, oxidation, and esterification. The PtCP functional nanolayer coating has the perpendicular nanosheet structure, which consists of needle-like morphologies with a size about 100 nm. The elemental X-ray maps and XRD data show that the topcoat layer is mainly amorphous aluminum oxide and the substrate layer is consisted of Ni and Ti. From the FT-IR and UV–Vis spectra, it is concluded that most of the PtCP molecules are bound up with the surface of Al_2O_3 coating through the carboxyl group. According to the indirect detection results of singlet oxygen generation, the steep decrease of DPBF absorption depending on the irradiation time indicates the efficient generation of $^1O_2$. Therefore, this PtCP functional nanolayer coating technology hopefully provides a new potential of this regimen as a possible alternative to prevent the microbism and the oxidative corrosion of the surface of NiTi alloy in future clinical applications.

Acknowledgment

This study was supported by a grant from the Korea Healthcare Technology R&D Project, Ministry for Health, Welfare & Family Affairs, Republic of Korea (A085136).

References

[1] T.J. Dougherty, C.J. Gomer, B.W. Henderson, G. Jori, D. Kessel, M. Korbelik, J. Moan, Q. Peng, J. Natl, Cancer Inst. 90 (1998) 889.
[2] T.J. Dougherty, J. Clin, Laser Med. Surg. 20 (2002) 3.
[3] M.R. Hamblin, T. Hasan, Photochem. Photobiol. Sci. 3 (2004) 436.
[4] G. Jori, C. Fabris, M. Soncin, S. Ferro, O. Coppellotti, D. Dei, L. Fantetti, G. Chiti, G. Roncucci, Lasers Surg. Med. 38 (2006) 468.
[5] C.J. Gomer, A. Ferrario, N. Hayashi, N. Rucker, B.C. Szirth, A.L. Murphree, Lasers Surg. Med. 8 (1988) 450.
[6] Y. Nitzan, B. Shainberg, Z. Malik, Curr. Microbiol. 19 (1989) 265.
[7] M. Ochsner, J. Photochem, Photobiol. B 39 (1997) 1.
[8] M. Wainwright, J. Antimicrob. Chemother. 42 (1998) 13.
[9] R.W. Redmond, J.N. Gamlin, Photochem. Photobiol. 70 (1999) 391.
[10] A.C. Moor, J. Photochem, Photobiol. B 57 (2000) 1.
[11] M. Wilson, J. Dobson, W. Harvey, Curr. Microbiol. 25 (1992) 77.
[12] Z. Jackson, S. Meghji, A. MacRobert, B. Henderson, M. Wilson, Lasers Med. Sci. 14 (1999) 150.

[13] S. Karrer, R.M. Szeimies, S. Ernst, C. Abels, W. Bäumler, M. Landthaler, Lasers Med. Sci. 14 (1999) 54.
[14] B. Zeina, J. Greenman, W.M. Purcell, B. Das, Br. J. Dermatol. 144 (2001) 274.
[15] M. Wainwright, J. Antimicrob. Chemother. 42 (1998) 13.
[16] T. Duerig, A. Pelton, D. Stockel, Mater. Sci. Eng. A 273 (1999) 149.
[17] D.A. Armitage, T.L. Parker, D.M. Grant, J. Biomed. Mater. Res. 66A (2003) 129.
[18] A. Kapanen, J. Ilvesaro, A. Danilov, J. Ryhanen, P. Lehenkari, J. Tuukkanen, Biomaterials 23 (2002) 645.
[19] K.-K. Wang, K.-H. Choi, H.-W. Shin, B.-J. Kim, J.-E. Im, S.-L. Oh, N.-S. Park, M. Jung, J.B. Oh, M.-J. Lee, H.K. Kim, Y.-R. Kim, Chem. Phys. Lett. 482 (2009) 81.
[20] J. Hu, I. Pavel, D. Moigno, M. Wumaier, W. Kiefer, Z. Chen, Y. Ye, Q. Wu, Q. Huang, S. Chen, F. Niu, Y. Gu, Spectrochim Acta A 59 (2003) 1929.
[21] M. Tonezzer, A. Quaranta, G. Maggioni, S. Carturan, G. Della Mea, Sens. Actuator B 122 (2007) 620.
[22] G. Maggioni, S. Carturan, M. Tonezzer, M. Buffa, A. Quaranta, E. Negro, G. Della Mea, Eur. Polym. J. 44 (2008) 3628.
[23] K. Nishio, N. Gokon, M. Hasegawa, Y. Ogura, M. Ikeda, H. Narimatsu, M. Tada, Y. Yamaguchi, S. Sakamoto, M. Abe, H. Handa, Colloid Surf. B 54 (2007) 249.
[24] D. Chen, D. Yang, J. Geng, J. Zhu, Z. Jiang, Appl. Surf. Sci. 255 (2008) 2879.
[25] P. Kubelka, F. Munk, Z. Tech. Phys. 12 (1931) 593.
[26] M. Fujii, M. Usui, S. Hayashi, E. Gross, D. Kovalev, N. Künzner, J. Diener, V.Y. Timoshenko, J. Appl. Phys. 95 (2004) 3689.
[27] T. Wilson, J. Am. Chem. Soc. 88 (1966) 2898.

Please cite this article as: K.-H. Choi, et al., Surf. Coat. Technol. (2010), doi:10.1016/j.surfcoat.2010.04.033